

Published in final edited form as:

*Clin Cancer Res.* 2009 November 1; 15(21): 6674–6682. doi:10.1158/1078-0432.CCR-09-0731.

## Quantifying anti-vascular effects of monoclonal antibodies to VEGF:

insights from multi-modality cross species imaging in colorectal cancer

James P B O'Connor<sup>1,2,\*</sup>, Richard A D Carano<sup>3,\*</sup>, Andrew R Clamp<sup>2,\*</sup>, Jed Ross<sup>3</sup>, Calvin C K Ho<sup>3</sup>, Alan Jackson<sup>1</sup>, Geoff J M Parker<sup>1</sup>, Chris J Rose<sup>1</sup>, Franklin V Peale<sup>4</sup>, Michel Friesenhahn<sup>5</sup>, Claire L Mitchell<sup>1,2</sup>, Yvonne Watson<sup>1</sup>, Caleb Roberts<sup>1</sup>, Lynn Hope<sup>2</sup>, Sue Cheung<sup>1</sup>, Hani Bou Reslan<sup>3</sup>, Mary Ann T Go<sup>6</sup>, Glenn J Pacheco<sup>6</sup>, Xiumin Wu<sup>7</sup>, Tim C Cao<sup>3</sup>, Sarajane Ross<sup>6</sup>, Giovanni A Buonaccorsi<sup>1</sup>, Karen Davies<sup>1</sup>, Jurjees Hasan<sup>2</sup>, Paula Thornton<sup>2</sup>, Olivia del Puerto<sup>8</sup>, Napoleone Ferrara<sup>7</sup>, Nicholas van Bruggen<sup>3</sup>, and Gordon C Jayson<sup>2</sup>

<sup>1</sup>Imaging Science and Biomedical Engineering, School of Cancer and Imaging Sciences, University of Manchester, Oxford Road, Manchester, M13 9PT, UK

<sup>2</sup>Cancer Research UK and University of Manchester Department of Medical Oncology, Christie Hospital, Wilmslow Road, Manchester, M20 4BX, UK

<sup>3</sup>Biomedical Imaging Group, Department of Tumor Biology and Angiogenesis, South San Francisco, California 94080, USA

<sup>4</sup>Department of Pathology, Genentech, Inc., South San Francisco, California 94080, USA

<sup>5</sup>Department of Biostatistics, Genentech, Inc., South San Francisco, California 94080, USA

<sup>6</sup>Department of Translational Oncology, Genentech, Inc., South San Francisco, California 94080, USA

<sup>7</sup>Ferrara Laboratory, Genentech, Inc., South San Francisco, California 94080, USA

<sup>8</sup>Roche Products Limited, 6 Falcon Way, Shire Park, Welwyn Garden City, AL7 1TW, UK

### Abstract

---

**Corresponding Author:** Dr James O'Connor PhD, Imaging Science and Biomedical Engineering, School of Cancer and Imaging Sciences, University of Manchester, Oxford Road, Manchester, M13 9PT, UK, Tel: +44 161 275 0040, Fax: +44 161 275 0003, james.o'connor@manchester.ac.uk

\*These authors contributed equally to this work

**Potential conflict of interest:** RAD Carano, J Ross, CCK Ho, FV Peale, M Friesenhahn, HB Reslan, MAT Go, GJ Pacheco, X Wu, TC Cao, S Ross, N Ferrara and N van Bruggen are all employees and stockholders with ownership interests in Genentech.

#### Statement of Translational Relevance

Dynamic contrast-enhanced MRI (DCE-MRI) can provide pharmacodynamic biomarkers of drug effect in studies of anti-angiogenic and anti-vascular agents. This technique is incorporated increasingly in early phase clinical trials of novel therapeutic agents. In this study of bevacizumab, we report DCE-MRI data that enhances current understanding of the temporal evolution of direct effects induced by anti-VEGF antibody therapy. In addition, we demonstrate how corroborative pre-clinical data can help distinguish between those DCE-MRI parameters that are sensitive to changes in tumor function and those that measure structure. These findings not only provide valuable insight into drug mechanism of action but also emphasize the need to optimize image timing and selection of analysis parameters when applying functional image techniques into clinical trials.

**Purpose**—Little is known concerning the onset, duration and magnitude of direct therapeutic effects of anti-VEGF therapies. Such knowledge would help guide the rational development of targeted therapeutics from bench to bedside and optimize use of imaging technologies that quantify tumor function in early phase clinical trials.

**Experimental design**—Pre-clinical studies were performed using ex vivo micro-CT and in-vivo ultrasound imaging to characterize tumor vasculature in a human HM-7 colorectal xenograft model treated with the anti-VEGF antibody G6-31. Clinical evaluation was by quantitative MRI in ten patients with metastatic CRC treated with bevacizumab.

**Results**—Micro-CT experiments demonstrated reduction in perfused vessels within 24-48 hours of G6-31 drug administration ( $p = 0.005$ ). Ultrasound imaging confirmed reduced tumor blood volume within the same time frame ( $p = 0.048$ ). Consistent with the pre-clinical results, reductions in enhancing fraction and fractional plasma volume were detected in patient CRC metastases within 48 hours after a single dose of bevacizumab that persisted throughout one cycle of therapy. These effects were followed by resolution of edema ( $p = 0.0023$ ) and tumor shrinkage in 9/26 tumors at day 12.

**Conclusion**—These data suggest that VEGF-specific inhibition induces rapid structural and functional effects with downstream significant anti-tumor activity within one cycle of therapy. This finding has important implications for the design of early phase clinical trials that incorporate physiological imaging. The study demonstrates how animal data help interpret clinical imaging data, an important step towards the validation of image biomarkers of tumor structure and function.

### Keywords

angiogenesis; biomarker; imaging; VEGF

### Introduction

Vascular endothelial growth factor (VEGF) plays a crucial role in angiogenesis by promoting endothelial cell proliferation, migration and vascular permeability. These effects enable tumor growth and survival (1, 2). Consequently, VEGF signaling has become an important target in drug development and has led to FDA approval of drugs that target either VEGF or the VEGF receptor (VEGFR) (3, 4). In particular, phase III trials of the humanized anti-VEGF monoclonal antibody bevacizumab (Avastin®; Genentech, San Francisco, CA) in combination with cytotoxic chemotherapeutics have shown improved overall survival in patients with metastatic colorectal cancer (CRC) (5) and non-small cell lung cancer (6). Improved progression free survival has also been reported in metastatic breast cancer (7).

These reports have led to rapid adoption of anti-VEGF therapies into clinical practice. This has been accompanied by interest in developing non-invasive image biomarkers that are sensitive to changes in the tumor microvasculature, since anti-VEGF therapies typically exhibit cytostatic rather than cytotoxic effects on tumor growth with little reduction in tumor size (8, 9). In particular, dynamic contrast enhanced magnetic resonance imaging (DCE-MRI) has been incorporated in early phase clinical trials of anti-VEGF antibody therapy (10,

11), tyrosine kinase inhibitors (TKI) (12, 13) and vascular disrupting agents (VDA) (14), to provide pharmacodynamic endpoints to assess drug activity.

At present, relatively little is known about the onset, magnitude, duration and temporal evolution of anti-VEGF therapy anti-vascular effects. Such information should have important implications for the rational development of targeted therapeutics and for the optimal design of future clinical trials incorporating physiological imaging endpoints (15, 16). To explore this issue, we performed clinical studies to evaluate the effects of bevacizumab in colorectal cancer (CRC) patients with liver metastases using DCE-MRI.

Corroborative data was provided from pre-clinical studies using x-ray micro-computed tomography (micro-CT) angiography, dynamic contrast-enhanced ultrasound (DCE-US) and histology in a CRC murine HM-7 xenograft model. The HM-7 model was chosen because of the strong response (based on tumor size) of this tumor cell line to anti-VEGF therapy and with the goal to better understand the vascular effects of a highly responsive tumor. Pre-clinical studies were performed with G6-31, a novel antibody to VEGF-A. G6-31 is a high affinity antibody to both murine and human VEGF-A, that has approximately 10 times greater binding affinity to human VEGF than A4.6.1 or the humanized version (bevacizumab). G6-31 has been shown to provide greater efficacy in pre-clinical xenograft models (including HM-7) than bevacizumab due to its ability to bind both tumor (human) and stromal (mouse) VEGF (17).

The primary aim of this study was to define the temporal evolution of anti-vascular effects induced during a single cycle of anti-VEGF mono-therapy. The secondary aim was to investigate whether cross-species imaging could provide insight into drug mechanism of action.

## Methods

### Pre-clinical study

**Animal Preparation**—The Genentech, Inc. AAALAC accredited review board approved all animal procedures. HM-7 human colon cancer cells ( $5 \times 10^6$  cells per animal) were implanted subcutaneously in the flanks of female athymic nude mice (Charles River Lab, Wilmington, MA). Mice weighed between 20 to 25 gm. Tumors were grown to between 100 to 300 mm<sup>3</sup> (where volume =  $0.5 \times \text{length} \times \text{width}^2$ ) at which point animals were enrolled into study.

**Micro-CT angiography time course study**—Forty one animals were randomized into two treatment groups. Animals received 5 mg/kg intra-venous (IV) (90 min study) or intra-peritoneal (IP) (24 and 48 hour studies) injection of either G6-31 or isotype control antibody. IV dosing was used for the 90 min study to maximize exposure over the 90 min of the experiment (17). Micro-CT angiography was used to measure vascular density in murine HM-7 xenografts, performed after animals were sacrificed at three time points: 90 min (G6-31, n = 6; control, n = 6), 24 hours (G6-31, n = 4; control, n = 4) and 48 hours (G6-31, n = 10; control, n = 11).

The micro-CT angiography methodology employed in this study has been described previously in detail (18). In brief, animals were perfused with MICROFIL® (Carver, MA) lead chromate latex immediately after sacrifice. The infused latex mixture was allowed to polymerize at room temperature for 60 minutes before tissue harvest. Dissected tumors were immersed in 10% neutral buffered formalin.

Tumors were then imaged with a  $\mu$ CT40 (SCANCO Medical, Basserdorf, Switzerland) system (tube 45 kV, current of 177  $\mu$ A, integration time 450 ms, isotropic resolution 16  $\mu$ m). An intensity threshold of 1195 Hounsfield Units (HU) and morphological filtering (erosion and dilation) were applied to the volumetric micro-CT image data to extract the vascular volume (VV). Tumor volume (TV) was extracted from the background in similar fashion with an intensity threshold of -8 HU. Vascular density was calculated as the ratio of VV to TV. Vascular and tumor intensity thresholds were determined by visual inspection of the segmentation results from a separate set of samples. Computations were performed by an in-house image analysis algorithm written in C++ and Python that employed the AVW image processing software library (AnalyzeDirect Inc., Lenexa, KS). Three-dimensional surface renderings were created from the micro-CT data with the use of Analyze 7.0 (AnalyzeDirect Inc., Lenexa, KS).

Tumors were then evaluated by MECA-32 histology. Formalin fixed, paraffin embedded tissue sections were de-paraffinized and pre-treated with Target Retrieval (Dako, Carpinteria, CA) at 99°C for 20 minutes. Quenching of endogenous peroxidase activity and blocking of endogenous biotin (Vector, Burlingame, CA) followed at room temperature. Sections were further blocked for 30 minutes with 10% normal rabbit serum in PBS with 3% BSA. Tissue sections were then incubated with rat anti-mouse panendothelial cell antigen, clone MECA-32, at 2  $\mu$ g/ml (BD Biosciences, San Jose, CA) for 60 minutes, biotinylated rabbit anti-rat at 2.5  $\mu$ g/ml (Vector) for 30 min, ABC reagent (Vector) for 30 minutes, followed by a 5-minute incubation in Metal Enhanced DAB (Pierce, Rockford, IL). Sections were counterstained with Mayer's hematoxylin. MECA-32-stained sections were analyzed with an Ariol SL-50 slide scanning platform (Applied Imaging; San Jose, CA), using a 10x objective to quantify vascular density. Tumor regions were identified and outlined manually. Pixel colors corresponding to MECA-32 staining were defined using a customized Metamorph software (Molecular Devices, Sunnyvale, CA) algorithm and vascular area was measured and normalized to tumor area.

**DCE-US and micro-CT angiography study**—Thirty eight animals were randomized into two treatment groups, control and G6-31 as follows: 4 hours (G6-31, n = 13; control, n = 13) and 48 hours (G6-31, n = 6; control, n = 6). Pre-treatment ultrasound imaging was performed to measure tumor volume. Animals then received 5 mg/kg intra-venous (4 hour study) or intra-peritoneal (48 hour study) injection of either G6-31 or isotype control antibody. IV dosing was used for the 4 hour study to maximize exposure over the 4 hours of the experiment. Ultrasound imaging was repeated 4 or 48 hours post-treatment, after which animals were sacrificed and micro-CT angiography was performed.

Mice were anesthetized using 2% isoflurane delivered in medical air at 1 l/s flow rate and placed supine on a dedicated small animal holding system (VisualSonics Inc., Toronto, ON,

Canada). Temperature was maintained at 37°C with a heated imaging platform. Body temperature and heart rate were monitored (THM 150, Indus Instruments, Houston, TX, USA). Imaging was performed with a Vevo 770 micro-imaging system (VisualSonics Inc., Toronto, Ontario, Canada) employing a single-element ultrasound transducer (center frequency 40 MHz, focal length 6 mm, axial resolution 40 µm, lateral resolution 100 µm).

Micro-bubble ultrasound contrast agent (Definity®, Bristol-Meyers Squibb Medical Imaging, Inc., Billerica, MA, USA) was administered as an intravenous bolus injection of 20 µl through a jugular vein puncture followed by a 20 µl saline flush. Single-slice B mode imaging was performed (center frequency 40 MHz, 50% power, axial resolution 40 µm, lateral resolution 100 µm, 20 frames per second). The ultrasound probe was aligned perpendicular to the animal and the tumor center was determined. 800 frames were acquired for first-pass kinetics analysis, the first 20 of which were acquired prior to contrast agent injection. These processes were performed in three planes (located within 1 mm of one another) and mean tumor area was calculated.

First-pass kinetics analysis of the signal intensity-time curve was employed to measure relative blood volume (rBV) and vascular transit time (VTT) for each pixel (19). Relative blood flow (rBF) was obtained for each pixel, where  $rBF = rBV/VTT$ . A lower limit perfusion threshold was determined from regions within the tumor that showed no enhancement after contrast agent administration. Mean rBV, rBF and VTT were determined for the perfused tumor tissue. Mean tumor area was calculated as the average area in three tumor planes: the center and +/- 1 mm from the center of the tumor. Each tumor area measurement was calculated from an average of 15 B-mode (pre-contrast) frames acquired prior to injection of microbubbles. The averaging of the pre-contrast images provided a high SNR image. The border of the tumor area was traced to exclude the skin, subcutaneous fat and muscle.

## Clinical Study

**Study design and patient selection**—Ethical approval was obtained from the Local Research Ethics Committee. Regulatory approval was granted by the UK Medicines and Healthcare Products Regulatory Agency. Ten patients with liver metastases from histology proven primary epithelial CRC and no previous cytotoxic chemotherapy exposure were recruited in an open label study. Written informed consent was obtained. Patients aged 18 years, with an Eastern Cooperative Oncology Group score between 0 and 2, and life expectancy of at least 3 months were eligible. All patients had at least one measurable lesion 2 cm present on three or more adjacent MRI slices and had no previous treatment with VEGF inhibitors or cytotoxic chemotherapy, or contraindications to VEGF inhibitors.

Patients received single agent 10 mg/kg bevacizumab (cycle 1) followed every two weeks by 10 mg/kg bevacizumab plus FOLFOX-6 (oxaloplatin/ 5FU/ leucovorin) for up to 6 months (cycles 2-13). MRI scans were performed during cycle 1 only, twice at baseline to establish parameter repeatability and then at 4 and 48 hours post-treatment and days 8 and 12.

**MRI data acquisition and analysis**—Data were acquired on a 1.5T Philips Inera system (Philips Medical Systems, Best, Netherlands). Anatomical pre-contrast  $T_1$ -weighted and  $T_2$ -weighted images were performed. Next, 75 axial  $T_1$ -weighted fast field echo volumes were consecutively-acquired every 4.97 s for a total of 6 min 13 s ( $TR$  4.0 ms,  $TE$  0.82 ms,  $\alpha = 20^\circ$ , one signal average, FOV of 375 mm  $\times$  375 mm, matrix 128  $\times$  128, 25 slices) following calculation baseline of  $T_1$  ( $\alpha = 2^\circ/10^\circ/20^\circ$ ; 4 signal averages; identical  $TR$ ,  $TE$ , imaging matrix). 0.1 mmol/kg of Omniscan (Amersham Health, Amersham, UK) was administered intravenously through a Spectris MR (Medrad Inc, Indianola, PA) power injector at 3 ml/s on the sixth dynamic time point. Slice thickness was 4 mm for small target lesions or 8 mm for larger lesions (superior-inferior coverage 100 mm or 200 mm). Finally, a post-contrast  $T_1$ -weighted image was acquired.

Regions of interest (ROI) were defined in 3D on the spatially co-registered high resolution  $T_1$ - and  $T_2$ -weighted volumes to encompass the entire tumor of interest. Whole tumor volume (WTV) was measured for each lesion. Voxels whose pre- and post-contrast agent time series had significantly different distributions (where  $p < 0.05$  on Mann-Whitney-Wilcoxon rank sum test) were classified as enhancing. The enhancing fraction ( $E_F$ ) was calculated by dividing the number of enhancing voxels by the total number of tumor voxels.

DCE-MRI data were analyzed using in-house software. Tumor  $T_1$  was calculated using the known relationship between the spoiled gradient echo signal,  $TR$ , flip angle and  $T_1$ . An arterial input function (AIF) was measured where possible; alternatively a population-derived function was applied (20) and the kinetic model parameters volume transfer constant ( $K^{trans}$ ), fractional volume of the extravascular extracellular space ( $v_e$ ) and fractional blood plasma volume ( $v_p$ ) were derived using the extended Tofts version of the Kety model. The model free parameter initial area under the gadolinium contrast agent concentration-time curve at 60 seconds ( $IAUC_{60}$ ) was also calculated (21). All parameters were calculated voxel-by-voxel. Median values of  $T_1$ ,  $K^{trans}$ ,  $v_e$  and  $IAUC_{60}$  and the mean  $v_p$  were determined from the enhancing portion of each tumor ROI.

### Statistical analysis

In the animal study, statistical analysis was performed with JMP statistical software package (SAS Institute Inc., Cary, NC, USA). Group comparisons for micro-CT and ultrasound metrics were evaluated with Student's t-test.  $p$  values less than 0.05 were considered significant.

In the clinical study, statistical analysis was performed using R (version 2.7.0). DCE-MRI data were analyzed on the logarithmically transformed scale. Repeatability was assessed using the replicate measurements available at baseline across patients. Reductions relative to baseline were based on results from random effects models where lesion-to-lesion effects within patients were included as random effects; separate random effects models were fit for each time point during treatment (4 hours, 48 hours, 8 days, and 12 days). Antilogs of the mean differences between baseline and time points during treatment were calculated to obtain relative changes from geomean baseline values expressed as percentages. Due to the large number of parameters analyzed,  $p$  values less than 0.01 were considered statistically

significant. All  $p$  values are two-tailed and were not formally adjusted for multiple comparisons.

## Results

### Ex vivo evidence for rapid G6-31 anti-vascular effects

Vascular density was measured using *ex vivo* micro-CT angiography along with corroborative histological measurements. We found statistically significant reductions in vascular density following G6-31 treatment compared with control animals at both 24 (G6-31 treated  $3.6 \pm 0.6$  %; control  $7.7 \pm 1.8$  %;  $p=0.005$ ) and 48 hours (G6-31 treated  $3.2 \pm 1.1$  %; control  $6.0 \pm 1.9$  %;  $p=0.0005$ ) (Figure 1A). Three dimensional micro-CT renderings exhibited a greatest reduction in central (core) tumor vasculature and a more modest effect in the peripheral vessels, which include co-opted host vasculature (Figure 1B).

MECA-32 histological analysis of the same animals confirmed significant reduction in vascular density to 40-50% of the levels observed in the control group at both 24 (G6-31 treated  $1.8 \pm 0.2$  %; control  $4.6 \pm 1.9$  %;  $p=0.032$ ) and 48 hours (G6-31 treated  $2.2 \pm 0.7$  %; control  $4.3 \pm 0.9$  %;  $p=0.00001$ ) (Figure 1C and Supplementary Figure). Vascular density estimates, measured by Micro-CT and MECA-32 staining were not significantly different from the control group at 90 minutes after G6-31 administration.

### In vivo evidence for rapid G6-31 anti-vascular effects

DCE-US studies were performed with the same animal model to determine if the above results were detectable *in vivo*. Subsequent *ex vivo* micro-CT measurements were also obtained. No differences were found in ultrasound estimates of rBV and rBF, or the micro-CT measurement of vascular density obtained 4 hours after G6-31 administration.

Tumor rBV was reduced in the G6-31 treated group relative to the control group at 48 hours post-treatment (G6-31 treated  $17.2 \pm 9.9$  %; control  $6.3 \pm 6.4$  %;  $p=0.048$ ). Tumor rBF exhibited a trend towards reduction in the G6-31 treated group at 48 hours (G6-31 treated  $18.4 \pm 13.3$  %; control  $7.9 \pm 4.8$  %;  $p=0.0991$ ) that was not statistically significant (Figure 2A). Micro-CT angiography analysis was performed following animal sacrifice and demonstrated significant reductions in vascular density for the G6-31 treated group relative to the control at 48 hours ( $p=0.003$ ). Ultrasound rBV parametric maps for G6-31 treated tumors exhibited a heterogeneous spatial pattern consistent with the vessel loss observed in the micro-CT data (Figure 2B, lower right image). These ultrasound data, along with the results from the micro-CT angiography time course study, demonstrate that a reduction in tumor rBV accompanies vessel loss following treatment with G6-31, suggesting that rBV is sensitive to structural change within tumor vasculature following anti-vascular therapy.

Mean tumor area was significantly increased in the control group compared to animals treated with G6-31 at both 4 (G6-31 treated  $0.27 \pm 4.7$  %; control  $5.1 \pm 4.4$  %;  $p=0.0125$ ) and 48 hours (G6-31 treated  $37.3 \pm 11.6$  %; control  $70.4 \pm 16.0$  %;  $p=0.00001$ ). These data suggest that structural changes in the tumor vasculature measured by endothelial cell staining, micro-CT and ultrasound lead to rapid growth stabilization. The detection of tumor growth suppression at 4 hours in the absence of statistically significant microvascular

changes may reflect the limitations of micro-CT and ultrasound in detecting small vascular differences that were more pronounced at 24-48 hours.

### **Clinical evidence for rapid anti-vascular effects induced by bevacizumab in human CRC metastases**

Reductions in  $v_p$  and  $E_F$  were detected throughout the cycle of bevacizumab. In particular, statistically significant reductions in tumor  $E_F$  were measured at 48 hours ( $p=0.004$ ) and maintained at days 8 ( $p=0.0005$ ) and 12 ( $p=0.0026$ ). These changes were accompanied by reductions in  $v_p$  at the corresponding time points (Table 1 and Figure 3). Representative parametric maps of enhancing voxels and  $v_p$  are shown (Figure 4A, B).

Vascular changes detected in human tumors at 48 hours concur with the above animal data. Rapid reductions in  $v_p$  indicate a loss of blood volume, consistent with the animal data detecting structural change in the tumor vasculature. In addition, the fraction of tumor that enhanced was significantly reduced (Table 1). A clear rim-core differential effect was observed as with the micro-CT data (Figure 4A, B). These changes then persisted throughout the cycle of bevacizumab therapy, confirming that significant anti-vascular effects occur rapidly in humans and then persist following anti-VEGF monoclonal antibody therapy. These data provide evidence that  $v_p$  and  $E_F$  are sensitive to structural changes induced by anti-vascular therapy and are useful parameters for interpreting dynamic contrast-enhanced imaging. Parameter within-subject co-efficient of variation was 7.1% for  $E_F$ , 15.4% for  $K^{trans}$ , 48.1% for  $v_p$  and 15.8% for  $T_1$ , showing comparable repeatability with the existing literature (22, 23).

In addition, we observed a statistically significant reduction of blood plasma volume 4 hours after bevacizumab administration ( $p = 0.0086$ ). This finding may represent a hyper-acute hemodynamic response at 4 hours in the human CRC metastases that differs from the sustained reduction (48 hours through to day 12) in blood plasma volume that accompanied later vessel loss. A hyperacute response was not observed in the HM-7 xenograft studies. One possible explanation for the lack of a hyper-acute hemodynamic response in the tumor xenograft model is that the HM-7 tumor vasculature is highly immature and lacks significant smooth muscle coverage (Unpublished observations by FV Peale). IV dosing was employed in these acute time point studies to maximize exposure over the short time period. It is unlikely that the negative results obtained at 90 min and 4 hrs could be due to the different route of administration since steady-state levels would be reached sooner with IV administration.

### **Bevacizumab induces change in $K^{trans}$ and $IAUC_{60}$ in human CRC metastases**

We found statistically significant decrease in median  $K^{trans}$  at 4 hours ( $p=0.0012$ ) following bevacizumab therapy which remained suppressed to day 8. These reductions were not sustained at day 12 (Table 1 and Figures 3 and 4C), suggesting that  $K^{trans}$  is more sensitive to functional changes in the tumor vasculature rather than structural changes. Example parameter maps are shown in Figure 4C. Change in median  $IAUC_{60}$  mirrored those of  $K^{trans}$  (data not shown).



The timing and magnitude of these changes are in keeping with previous clinical trials of anti-VEGF antibodies (10) and TKI (12, 24, 25). However, changes in  $K^{trans}$  and  $IAUC_{60}$  are difficult to interpret.  $IAUC_{60}$  is relatively easy to calculate and repeatable but is not physiologically specific.  $K^{trans}$  is a composite estimate of both the blood flow and the permeability-surface area product per unit volume of tissue for trans-endothelial transport between plasma and extravascular space (26). The observed initial reductions in  $K^{trans}$  are, therefore, consistent both with an initial decrease in blood flow and/or a reduction in vessel permeability. This difficulty in interpretation is an important factor when the analysis of dynamic contrast-enhanced imaging data is restricted to physiologically non-specific parameters.

### **Evidence that bevacizumab induces edema resolution and tumor shrinkage**

Reduction in tumor volume was detected across the cohort of 26 tumors by day 12 (Figure 5A) although this change did not reach statistical significance ( $p = 0.0569$ ). No patients achieved partial response as defined by RECIST. Based on the replicate observations taken at baseline, 95% of ratios of serial measurements of tumor volume are estimated to be between 76.2% and 131.3%. Using these criteria, 9 out of 26 tumors (in five different patients) exhibited statistically significant volume reduction (Figure 5B).

Reductions in tumor volume were accompanied by statistically significant reductions in tumor pre-contrast  $T_1$  from baseline to day 12 ( $p = 0.0023$ ) (Figures 4D and 5A), likely to represent resolution of tumor edema caused by reduced vascular permeability. This mirrors similar rapid resolution of edema observed following inhibition of VEGF with tyrosine kinase inhibitor AZD2171 in glioblastoma multiforme (27). Although a small cytotoxic effect secondary to the early anti-vascular effects of bevacizumab cannot be discounted, these data support the hypothesis that bevacizumab-induced reduction in vascular permeability and blood flow leads to reduced tumor tissue edema, accompanied by reduction in tumor volume.

## **Discussion**

Physiological imaging can provide detailed quantitative information concerning tumor biology and drug mechanism of action, that may help guide the rational development of targeted therapeutics (16). We have presented valuable new information concerning the temporal evolution of anti-vascular effects induced by anti-VEGF antibodies that has important implications for studies that evaluate anti-vascular or anti-angiogenic agents.

### **Insight into drug mechanism of action**

Previous studies have shown rapid reductions in vascular permeability. In one study, Berry et al found that 24 hours after treatment with G6-31  $K^{trans}$  was reduced 62% in the same HM-7 xenograft model that was employed in this paper (28). Our current results demonstrate that micro-CT angiography, a technique employed previously to characterize normal tissue and tumor vasculature (18) can detect rapid vessel loss in murine HM-7 xenografts within the first 24 hours following treatment with G6-31. This is the first study to show that an anti-VEGF therapy can reduce tumor vascular density within such a short time

frame. These changes were accompanied by reductions in blood volume, observed at 48 hours using DCE-US.

These data (measurements of blood volume and vascular density) reflect structural changes in tumor vasculature following anti-VEGF therapy and help interpret the clinical DCE-MRI data (measurements of fractional blood plasma volume and proportional tumor enhancement) at 48 hours after bevacizumab administration in metastatic CRC. Further DCE-MRI data at 8 and 12 days provide evidence that these effects, likely to be structural, are maintained throughout a two-week cycle of bevacizumab and lead to resolution of tumor edema and decrease in tumor volume.

In distinction, the parameters  $K^{\text{trans}}$  and  $IAUC_{60}$  showed transient reductions from baseline values that were lost by the end of the cycle of anti-VEGF therapy. Both  $K^{\text{trans}}$  and  $IAUC_{60}$  reflect a combination of blood flow and capillary permeability, suggesting that these parameters are sensitive to transient functional changes in the tumor vasculature and that measurement timing is critical in order to detect these changes induced by anti-VEGF therapy.

Overall, these data provide evidence that the structural and functional changes induced by anti-VEGF monoclonal antibodies lead to rapid downstream effects in tumor morphology. Growth stabilization was demonstrated within 48 hours in murine HM-7 xenografts treated with G6-31, relative to controls. In the clinical data, CRC liver metastases showed statistically significant reduction in  $T_1$ , consistent with resolution in edema that was accompanied by a trend towards volume reduction across the group of metastases. In 9/26 lesions, the volume reduction was statistically significant. Taken together, these data provide cross-species evidence for anti-vascular effect with anti-VEGF antibodies within 48 hours, with resultant rapid resolution of edema and tumor shrinkage.

There are several limitations to this study that qualify the above conclusions. For the preclinical study, a single xenograft model was evaluated by employing multiple imaging modalities and time points. The extensive evaluation of a single responsive model does not provide a thorough evaluation of the magnitude of the vascular imaging response as a function of the responsiveness of the tumor. This would require the evaluation of number of additional models that represent a range (including a non-responder) of responsiveness based on tumor volume. This would likely provide additional insight into the range of the vascular response and answer the question of the state of these vascular imaging parameters in a non-responding tumor. It would also be of value to evaluate a model of liver metastases, where tumors would likely experience a more representative micro-environment to that experience by clinical CRC liver metastases. Although these are interesting questions, they are beyond the scope of this study which focused on quantifying the vascular response of a tumor model where there is a potent anti-VEGF response as a means to better understand the vascular changes associated with the positive DCE-MRI response that has been observed in clinical anti-VEGF studies. For the clinical study, the temporal resolution of the DCE-MRI study was not sufficient to obtain independent estimates of blood flow and permeability.

## Choice of physiological imaging biomarkers in clinical trials

Traditional clinical trial assessment of tumor response has relied on codified radiological response criteria (29, 30). In RECIST, a categorical measurement of treatment response is provided where *partial response* is defined as greater than 30% reduction in the longest diameter of the sum of all marker lesions, which equates to around 65% reduction in tumor volume (31). Using this approach, anti-vascular and anti-angiogenic agents have been considered to induce insignificant changes in tumor size (8). This has stimulated considerable interest in the serial non-invasive evaluation of the tumor microenvironment in early phase clinical trials of targeted therapeutics.

DCE-MRI and dynamic contrast enhanced CT (DCE-CT) have been used to estimate tumor blood flow, blood volume and edema and provide pharmacodynamic endpoints of drug activity in around thirty phase I/II clinical trials of anti-VEGF antibodies, TKI and VDA. Nearly all of these studies have reported either  $K^{\text{trans}}$  or  $IAUC_{60}$  as primary endpoints in line with consensus recommendations (32). However, these parameters have equivocal and complex physiological meanings (9). This study demonstrates the value of using multi-parametric analyses that includes tumor  $T_1$ ,  $E_F$  and multiple modeled parameter endpoints that includes  $v_p$ , rather than  $K^{\text{trans}}$  and/or  $IAUC_{60}$  alone. Such an approach enables changes in both the tumor vascular structure and function to be detected.

This study demonstrates that measuring tumor size may yield important information in studies of some targeted therapeutic agents, when size change is assessed as a continuous (rather than categorical) variable. This finding concurs with previous reports in patients with metastatic renal cell cancer receiving sorafenib (33), suggesting that tumor size should remain an important metric for evaluating drugs that induce changes in blood flow and vascular permeability. In practice, it may be the combination of biomarkers based on tumor size, morphology and function that provides the most useful evaluation of targeted therapeutics in early phase clinical development.

## Importance of measurement timing in image analysis

We have reported DCE-MRI data that quantify the temporal evolution of the anti-vascular effects of bevacizumab. To date, imaging studies have neither optimized scan timing nor had sufficient frequency of examination to accurately characterize the pharmacodynamic properties of novel therapies (9, 34). Rapid anti-VEGF antibody mediated anti-vascular effects have been reported in animal models (35), but the temporal evaluation of bevacizumab-induced anti-vascular effects in humans has not been performed previously. In comparable studies, DCE-MRI measurements have been performed at around 4 hours post-dosing to evaluate VDA (14) and around 24-48 hours post-therapy to evaluate TKI (25, 27). Studies of bevacizumab have limited imaging endpoints to late time points in the treatment cycle; patients were imaged at 7-12 days following two weekly bevacizumab mono-therapy in CRC assessed by DCE-CT (36) and at the end of a three week cycle in a DCE-MRI study of inflammatory breast cancer (11).

In this clinical study, we chose imaging time points at 4 and 48 hours (consistent with the ex vivo and in vivo animal studies, and with trials of VDA and TKI) and day 12 (bevacizumab

has been reported previously to impair blood flow and blood volume at this time in CRC (36). An additional time point was selected at day 8, since pre-clinical evidence has suggested that vascular normalization may occur within a week following administration of a VEGF receptor inhibitor (37). Our results demonstrate a complex temporal evolution of parameter change that underpins the interaction of tumor biology and drug mechanism of action and demonstrates how pharmacodynamic biomarkers may be used to optimize evaluation of novel therapies (34). These results support the use of detailed physiological imaging in small phase I/II studies of anti-vascular and anti-angiogenic agents to define the optimum timing and frequency of image acquisition for large phase II and all phase III trials of the same agents, where practical and economic reasons limit the amount of imaging that may be incorporated.

Lack of validation is a major factor that limits wider acceptance and application of physiological imaging such as DCE-MRI and DCE-CT to clinical studies of anti-vascular and anti-angiogenic compounds. This study highlights the benefits of multi-modality imaging in evaluating mechanism of drug action and how animal data using combined imaging and histology may help to interpret clinical imaging techniques. However, considerable further studies are required to validate the physiological imaging biomarkers described in this study.

## Supplementary Material

Refer to Web version on PubMed Central for supplementary material.

## Acknowledgments

We thank Jeffrey Eastham-Anderson for developing the Metamorph algorithms, managing the histological imaging and automated image analysis of MECA-32-stained tumor samples and Greg Plowman for his comments on the manuscript.

**Financial support:** This work was supported by Roche Products Ltd.; and by *Cancer Research UK* [Grant C19221/A6086 to JPBO'C].

## References

1. Senger DR, Galli SJ, Dvorak AM, et al. Tumor cells secrete a vascular permeability factor that promotes accumulation of ascites fluid. *Science*. 1983; 219:983–985. [PubMed: 6823562]
2. Leung DW, Cachianes G, Kuang WJ, Goeddel DV, Ferrara N. Vascular endothelial growth factor is a secreted angiogenic mitogen. *Science*. 1989; 246:1306–1309. [PubMed: 2479986]
3. Ferrara N, Gerber HP, LeCouter J. The biology of VEGF and its receptors. *Nat Med*. 2003; 9:669–676. [PubMed: 12778165]
4. Kerr DJ. Targeting angiogenesis in cancer: clinical development of bevacizumab. *Nat Clin Pract Oncol*. 2004; 1:39–43. [PubMed: 16264798]
5. Hurwitz H, Fehrenbacher L, Novotny W, et al. Bevacizumab plus irinotecan, fluorouracil, and leucovorin for metastatic colorectal cancer. *N Engl J Med*. 2004; 350:2335–2342. [PubMed: 15175435]
6. Sandler A, Gray R, Perry MC, et al. Paclitaxel-carboplatin alone or with bevacizumab for non-small-cell lung cancer. *N Engl J Med*. 2006; 355:2542–2550. [PubMed: 17167137]
7. Miller K, Wang M, Gralow J, et al. Paclitaxel plus bevacizumab versus paclitaxel alone for metastatic breast cancer. *N Engl J Med*. 2007; 357:2666–2676. [PubMed: 18160686]

8. Ratain MJ, Eckhardt SG. Phase II studies of modern drugs directed against new targets: if you are fazed, too, then resist RECIST. *J Clin Oncol.* 2004; 22:4442–4445. [PubMed: 15483011]
9. O'Connor JP, Jackson A, Parker GJ, Jayson GC. DCE-MRI biomarkers in the clinical evaluation of antiangiogenic and vascular disrupting agents. *Br J Cancer.* 2007; 96:189–195. [PubMed: 17211479]
10. Jayson GC, Zweit J, Jackson A, et al. Molecular imaging and biological evaluation of HuMV833 anti-VEGF antibody: implications for trial design of antiangiogenic antibodies. *J Natl Cancer Inst.* 2002; 94:1484–1493. [PubMed: 12359857]
11. Wedam SB, Low JA, Yang SX, et al. Antiangiogenic and antitumor effects of bevacizumab in patients with inflammatory and locally advanced breast cancer. *J Clin Oncol.* 2006; 24:769–777. [PubMed: 16391297]
12. Drevs J, Siegert P, Medinger M, et al. Phase I clinical study of AZD2171, an oral vascular endothelial growth factor signaling inhibitor, in patients with advanced solid tumors. *J Clin Oncol.* 2007; 25:3045–3054. [PubMed: 17634482]
13. Hahn OM, Yang C, Medved M, et al. Dynamic contrast-enhanced magnetic resonance imaging pharmacodynamic biomarker study of sorafenib in metastatic renal carcinoma. *J Clin Oncol.* 2008; 26:4572–4578. [PubMed: 18824708]
14. Galbraith SM, Maxwell RJ, Lodge MA, et al. Combretastatin A4 phosphate has tumor antivascular activity in rat and man as demonstrated by dynamic magnetic resonance imaging. *J Clin Oncol.* 2003; 21:2831–2842. [PubMed: 12807936]
15. Workman P, Aboagye EO, Chung YL, et al. Minimally invasive pharmacokinetic and pharmacodynamic technologies in hypothesis-testing clinical trials of innovative therapies. *J Natl Cancer Inst.* 2006; 98:580–598. [PubMed: 16670384]
16. O'Connor JP, Jackson A, Asselin MC, et al. Quantitative imaging biomarkers in the clinical development of targeted therapeutics: current and future perspectives. *Lancet Oncol.* 2008; 9:766–776. [PubMed: 18672212]
17. Liang WC, Wu X, Peale FV, et al. Cross-species vascular endothelial growth factor (VEGF)-blocking antibodies completely inhibit the growth of human tumor xenografts and measure the contribution of stromal VEGF. *J Biol Chem.* 2006; 281:951–961. [PubMed: 16278208]
18. Shojaei F, Wu X, Zhong C, et al. Bv8 regulates myeloid-cell-dependent tumour angiogenesis. *Nature.* 2007; 450:825–831. [PubMed: 18064003]
19. Schwarz KQ, Bezante GP, Chen X, Mottley JG, Schlieff R. Volumetric arterial flow quantification using echo contrast. An in vitro comparison of three ultrasonic intensity methods: radio frequency, video and Doppler. *Ultrasound Med Biol.* 1993; 19:447–460. [PubMed: 8236587]
20. Parker GJ, Roberts C, Macdonald A, et al. Experimentally-derived functional form for a population-averaged high-temporal-resolution arterial input function for dynamic contrast-enhanced MRI. *Magn Reson Med.* 2006; 56:993–1000. [PubMed: 17036301]
21. Tofts PS. Modeling tracer kinetics in dynamic Gd-DTPA MR imaging. *J Magn Reson Imaging.* 1997; 7:91–101. [PubMed: 9039598]
22. Jackson A, Jayson GC, Li KL, et al. Reproducibility of quantitative dynamic contrast-enhanced MRI in newly presenting glioma. *Br J Radiol.* 2003; 76:153–162. [PubMed: 12684231]
23. Evelhoch JL, LoRusso PM, He Z, et al. Magnetic resonance imaging measurements of the response of murine and human tumors to the vascular-targeting agent ZD6126. *Clin Cancer Res.* 2004; 10:3650–3657. [PubMed: 15173071]
24. Morgan B, Thomas AL, Drevs J, et al. Dynamic contrast-enhanced magnetic resonance imaging as a biomarker for the pharmacological response of PTK787/ZK 222584, an inhibitor of the vascular endothelial growth factor receptor tyrosine kinases, in patients with advanced colorectal cancer and liver metastases: results from two phase I studies. *J Clin Oncol.* 2003; 21:3955–3964. [PubMed: 14517187]
25. Liu G, Rugo HS, Wilding G, et al. Dynamic contrast-enhanced magnetic resonance imaging as a pharmacodynamic measure of response after acute dosing of AG-013736, an oral angiogenesis inhibitor, in patients with advanced solid tumors: results from a phase I study. *J Clin Oncol.* 2005; 23:5464–5473. [PubMed: 16027440]

26. Tofts PS, Brix G, Buckley DL, et al. Estimating kinetic parameters from dynamic contrast-enhanced T(1)-weighted MRI of a diffusable tracer: standardized quantities and symbols. *J Magn Reson Imaging*. 1999; 10:223–232. [PubMed: 10508281]
27. Batchelor TT, Sorensen AG, di Tomaso E, et al. AZD2171, a pan-VEGF receptor tyrosine kinase inhibitor, normalizes tumor vasculature and alleviates edema in glioblastoma patients. *Cancer Cell*. 2007; 11:83–95. [PubMed: 17222792]
28. Berry LR, Barck KH, Go MA, et al. Quantification of viable tumor microvascular characteristics by multispectral analysis. *Magn Reson Med*. 2008; 60:64–72. [PubMed: 18421695]
29. World Health Organization. WHO handbook for reporting results of cancer treatment. World Health Organization; Geneva: 1979.
30. Therasse P, Arbuck SG, Eisenhauer EA, et al. European Organization for Research and Treatment of Cancer; National Cancer Institute of the United States; National Cancer Institute of Canada. New guidelines to evaluate the response to treatment in solid tumors. *J Natl Cancer Inst*. 2000; 92:205–216. [PubMed: 10655437]
31. Padhani AR, Ollivier L. The RECIST (Response Evaluation Criteria in Solid Tumors) criteria: implications for diagnostic radiologists. *Br J Radiol*. 2001; 74:983–986. [PubMed: 11709461]
32. Leach MO, Brindle KM, Evelhoch JL, et al. The assessment of antiangiogenic and antivascular therapies in early-stage clinical trials using magnetic resonance imaging: issues and recommendations. *Br J Cancer*. 2005; 92:1599–1610. [PubMed: 15870830]
33. Karrison TG, Maitland ML, Stadler WM, Ratain MJ. Design of phase II cancer trials using a continuous endpoint of change in tumor size: application to a study of sorafenib and erlotinib in non small-cell lung cancer. *J Natl Cancer Inst*. 2007; 99:1455–1461. [PubMed: 17895472]
34. Jain RK, Duda DG, Willett CG, et al. Biomarkers of response and resistance to antiangiogenic therapy. *Nat Rev Clin Oncol*. 2009; 6:327–338. [PubMed: 19483739]
35. Yuan F, Chen Y, Dellian M, et al. Time-dependent vascular regression and permeability changes in established human tumor xenografts induced by an anti-vascular endothelial growth factor/vascular permeability factor antibody. *Proc Natl Acad Sci U S A*. 1996; 93:14765–14770. [PubMed: 8962129]
36. Willett CG, Boucher Y, di Tomaso E, et al. Direct evidence that the VEGF-specific antibody bevacizumab has antivascular effects in human rectal cancer. *Nat Med*. 2004; 10:145–147. [PubMed: 14745444]
37. Winkler F, Kozin SV, Tong RT, et al. Kinetics of vascular normalization by VEGFR2 blockade governs brain tumor response to radiation: role of oxygenation, angiopoietin-1, and matrix metalloproteinases. *Cancer Cell*. 2004; 6:553–563. [PubMed: 15607960]

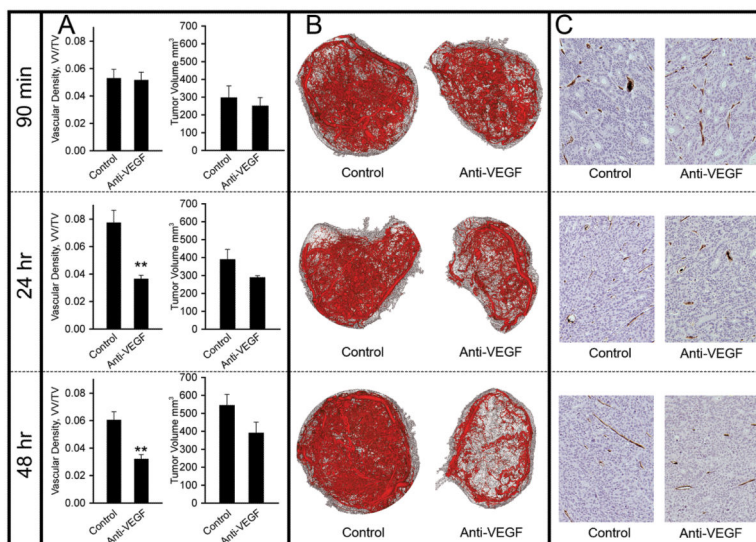


**Figure 1. Ex-vivo evidence for rapid anti-vascular effects of G6-31**

(A) Change in vascular density (VV/TV), as measured by micro-CT at 90 min, 24 hours and 48 hours in control animals and those treated with the anti-VEGF antibody G6-31.

(B) Representative micro-CT angiographic data for each treatment group at 90 min and at 24 and 48 hours. Extracted vascular network (red) and entire tumor (gray) are shown.

(C) Histological sections stained with MECA-32 for corresponding time points. Note that the brown intravascular pigment is micro-CT lead chromate contrast agent, which only partially fills vessel lumens after histological processing. Vessel area was measured by assessing DAB-stained endothelium at the vessel perimeter. See supplemental Figure 1 for the corresponding segmented images.

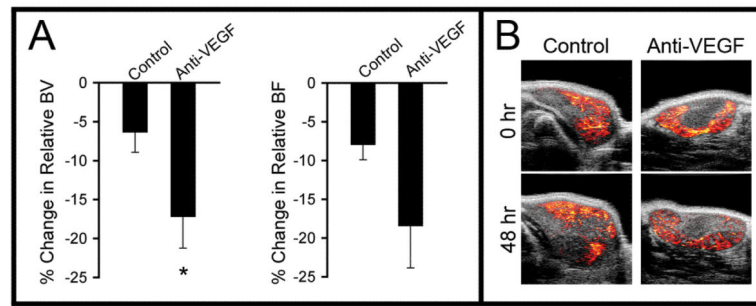


**Figure 2. In-vivo evidence for reduction in relative blood volume following G6-31**  
(A) Percentage change in relative blood volume (rBV) and relative blood flow (rBF) in control and treated groups after 48 hours of anti-VEGF treatment.  
(B) Representative ultrasound perfusion blood volume maps for each treatment group pre-treatment and at 48 hrs post-treatment.



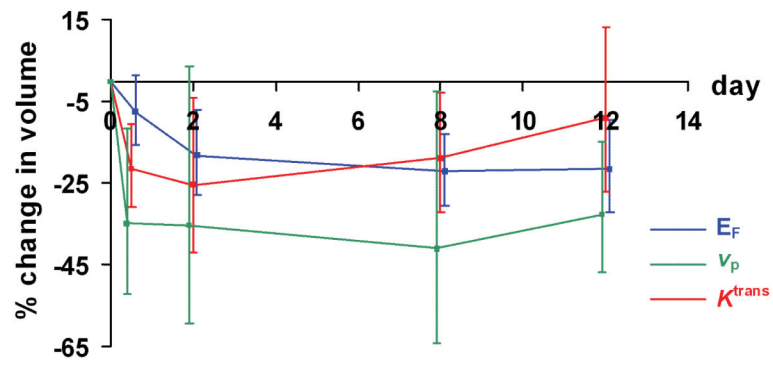


**Figure 3. In vivo evidence of the temporal evolution of anti-vascular effects of bevacizumab** Measurements of enhancing fraction ( $E_F$ ), mean blood plasma volume ( $v_p$ ) and median volume transfer constant ( $K^{trans}$ ) in 26 tumors; error bars indicating the 95% confidence intervals for point estimates of log drops.

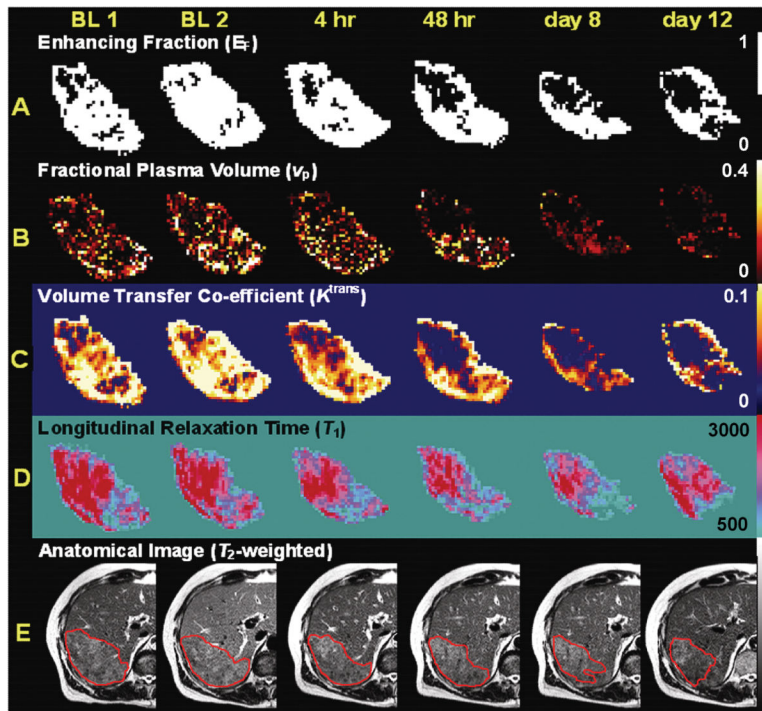


**Figure 4. Representative MRI parameter maps from one patient**

(A) Map of enhancing voxels shows a significant decrease beginning at 48 hours that persists through to day 12. Note that the loss of central enhancement.

(B) Maps of fractional blood plasma volume ( $v_p$ ) also shows a significant decrease, here beginning at 4 hours that persists through to day 12.

(C) Maps of the volume transfer constant ( $K^{trans}$ ) show reduction in parameter within 4 hours that persist at 48 hours and day 8, but return to baseline levels by day 12. These changes are consistent with reduction in either vessel permeability and/or blood flow.

(D) Maps of the longitudinal relaxation time ( $T_1$ ) measured prior to contrast agent administration show a clear progressive reduction in  $T_1$ , a measurement of tumor edema.

(E)  $T_2$ -weighted anatomical image without contrast (arbitrary signal intensity units). All parameter maps and images were obtained at baseline twice (Base 1 and Base 2) and at 4 hours, 48 hours, 8 days and 12 days after bevacizumab administration. Tumors region of interest are outlined in red and show gradual reduction in tumor size.

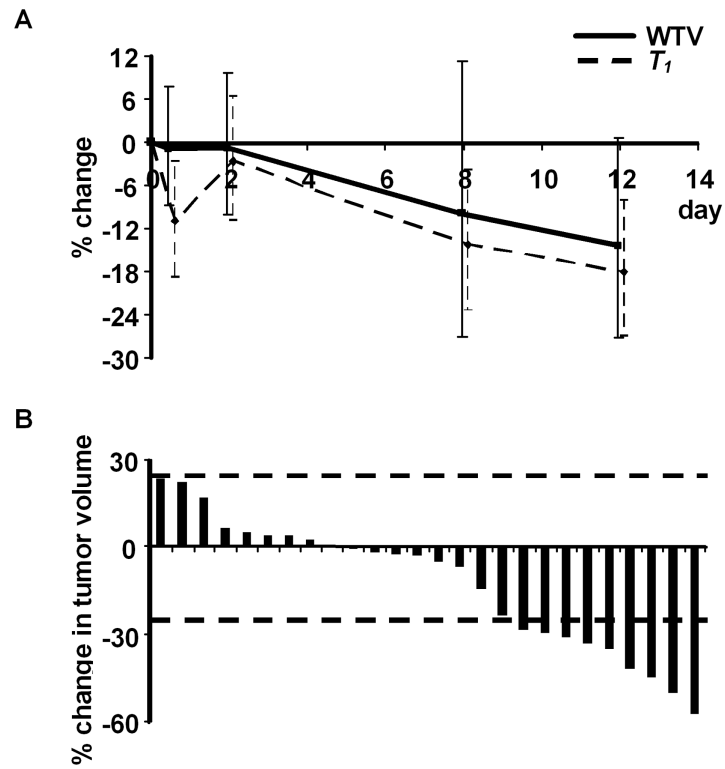


**Figure 5. Evidence for reduction in tumor size with bevacizumab mono-therapy**

(A) Temporal evolution of tumor volume reduction and change in longitudinal relaxation time ( $T_1$ ) from baseline through to day 12 in 26 tumors.

(B) Waterfall plots demonstrate percentage reduction in tumor volume from baseline size at day 12. The dotted lines denote lesions that changed in size by greater than the lower and upper limits of 95% of serial parameter ratios.

**Table 1**

Percentage change in enhancing fraction ( $E_F$ ), DCE-MRI parameters, longitudinal relaxation time ( $T_1$ ) and whole tumor volume (WTV) measured from baseline (BL) to four post-treatment time points (4 and 48 hours and days 8 and 12). Mean values of percentage change and 95% confidence intervals are expressed.  $p$  values are two tailed, considered significant when less than 0.01 and were calculated using the mixed effects model on logarithmically transformed data

Parameter	BL to 4 hours		BL to day 48 hours		BL to day 8		BL to day 12	
	%	p value	%	p value	%	p value	%	p value
$E_F$	-7.5	0.0913	-18.1	0.0040	-22.2	0.0005	-21.6	0.0026
	-15.7 to 1.4		-27.9 to -7.1		-30.4 to -13.0		-32.1 to -9.6	
$v_p$	-34.9	0.0086	-35.2	0.0678	-40.9	0.0410	-32.7	0.0027
	-52.0 to -11.7		-59.5 to 3.6		-64.2 to -2.5		-46.7 to -15.0	
$K^{trans}$	-21.3	0.0012	-25.5	0.0243	-18.9	0.0260	-9.0	0.3719
	-30.8 to -10.5		-42.0 to -4.2		-32.0 to -3.0		-27.0 to 13.4	
$v_e$	-4.0	0.5337	-5.9	0.3132	-13.3	0.0785	-6.8	0.5393
	-16.3 to 10.1		-16.8 to 6.5		-26.2 to -1.9		-26.9 to 18.6	
$T_1$	-11.0	0.0146	-0.3	0.5374	-14.2	0.0129	-18.1	0.0023
	-18.7 to -2.6		-10.9 to 6.4		-23.5 to -3.9		-26.9 to -8.1	
WTV	-0.9	0.8218	-0.8	0.8704	-9.9	0.3015	-14.5	0.0569
	-8.9 to 7.8		-10.2 to 9.7		-27.1 to 11.3		-27.2 to 0.5	